06

Electronic mechanism of propagation of nanosecond breakdown channel in liquid organic dielectrics

© R.V. Emlin,[1] I.F. Punanov,[1] V.D. Kulikov[2]

[1] Institute of Electrophysics, Ural Branch, Russian Academy of Sciences,
Yekaterinburg, Russia
[2] Tomsk Agricultural Institute,
Tomsk, Russia
e-mail: ivan.punanov@gmail.com

Received April 11, 2022
Revised May 24, 2022
Accepted May 28, 2022

The mechanism of anode-initiated breakdown in liquid organic dielectrics with long molecular chains is proposed on the basis of the experimental data on high velocities of the breakdown channel propagation in organosilicon and organofluorine liquids ($\sim 10^7$ cm/s), which are comparable to those obtained earlier in crystals in the same conditions. The high velocities of the anode-initiated breakdown channels are satisfactorily explained within the model of the cascade Auger transitions, developed for the crystalline materials. According to this model, velocity of the breakdown channel propagation is proportional to the electrical field strength. The time delay in breakdown channel formation relative to the voltage pulse rise time does not exceed $\sim 5 \cdot 10^{-10}$ s within the margin of error.

Keywords: electrical breakdown in liquid, nanosecond breakdown, breakdown mechanism.

DOI: 10.21883/TP.2022.10.54361.93-22

Introduction

Modern trends in the pulsed power are associated with the development of high-power facilities [1–3], the voltage in which reaches several megavolts. In such facilities insulating materials are exposed to strong pulsed electric fields $\sim 10^8$ V/cm in the time range of $\sim 10^{-7}-10^{-9}$ s. Due to electromagnetic energy compression, the intensity of energy impact on materials can reach 10^{23} W/cm^2 [4]. One of the most important tasks during the development of such facilities is to increase the reliability of insulation, in particular, to prevent the breakdown of dielectric units and media under exposure of extreme electric fields. On the other hand, there are devices where breakdown is the basis of their functioning, for example, solid dischargers [5]. Both the problems of breakdown prevention and the problems of insulation coordination and control of the breakdown process require a deep understanding of the fundamental physical mechanisms of the breakdown process in various condensed media — crystalline, ceramic, liquid.

Significant progress was made in the study of the electrical breakdown mechanisms of crystalline materials due to the well-developed theory of solids. Understanding of the breakdown mechanisms of liquid dielectrics is associated with difficulties, which include the insufficiently developed theory of matter in the liquid phase, the absence of long-range order in liquid, the inevitable presence of impurities in samples, etc. [6]. Despite these difficulties, researchers developed a significant number of theories of breakdown initiation in liquid dielectrics. However, even given the variety of works, only two fundamentally different physical mechanisms for the development of electrical breakdown in liquids are currently being considered: the so-called „bubble“ and „ionization“ mechanisms [7–10].

The ionization mechanism assumes the occurrence of a conducting channel in liquid as a result of ionization of molecules due to field ionization (anode-initiated) or impact ionization by electrons (cathode-initiated). The bubble mechanism is a process of rapid local heating of liquid by injection currents in the near-electrode regions, boiling and vaporing, further ionization of vapor-gas cavities, and the beginning of the plasma channel formation. The ionization mechanism of breakdown manifests itself in the form of propagation of „fast“ conducting channels from the anode, whereas the bubble one — „slower“ channels from the cathode.

The literature shows a significant difference between these two processes. In particular, in liquid dielectrics the velocity of the anode-initiated breakdown front (v_a) is much higher than the velocity of the cathode-initiated one (v_c). The velocity v_a increases with the applied voltage increasing, as well as in the process of propagation of the tip of the breakdown channel to the negative electrode. For example, the values of v_a and v_c in n-heptane at a voltage of ~ 30 kV and the electrode gap length of ~ 10 mm according to the photochronometric data are $3.4 \cdot 10^5$ and $2.2 \cdot 10^4$ cm/s, respectively [11]. Under close experimental conditions at a voltage of ~ 40 kV and a gap length of ~ 5 mm by the method of photoelectronic scanning of the luminescence of channels for transformer oil the values of the velocities v_a and v_c equal to $2.5 \cdot 10^5$ and $8 \cdot 10^4$ cm/s [12] were obtained. For reliable initiation of only „fast“ anode-associated channels, the „point–plane“ electrode configuration with a positive needle is used, which

provides a rather heterogeneous strong field around the anode.

Previously, it was shown that the features of the anode-initiated breakdown in alkali halide crystals [13,14], quartz [15], cadmium sulfide [16], polyethylene [17], namely — high velocity of the channel front $\sim 10^7-10^8$ m/s, breakdown current density $\sim 10^4$ A/cm^2, the crystallographic orientation of breakdown channels — are satisfactorily described by a mechanism based on cascade Auger transitions in the valence band of the dielectric. The observed similarity between the dynamics of anode-initiated breakdown channels formation in ion-covalent crystals, polymeric dielectrics [18–20] and in dielectric liquids [7,8] allows us to conclude that they can be caused by the same fundamental physical processes. This conclusion makes it possible to obtain theoretical estimates of the measured parameters of the breakdown process in dielectric liquids using the approach developed earlier for dielectric crystals [13–15].

To implement this theoretical model, it is necessary that the dielectric be locally exposed to a strong electric field ($\sim 10^8$ V/cm). Such a strength can be achieved at the microprotrusions of the anode, as well as at the tip of the breakdown channel during its growth. However, the high field strength at the microprotrusions plays a role only if the shunting effect of surface currents is minimized. For this, it is necessary that the field growth rate be about 10^{12} V/s. This condition is satisfied if high-pressure gas spark gap is used in the pulse generation circuit, which provides subnanosecond voltage rise times [21].

In this paper the experimental results on the velocity of the anode-initiated breakdown front in liquid dielectrics (organofluorine and organosilicon liquids, transformer oil, ethanol) under nanosecond exposure to voltage pulses with a width of $\sim 10^{-8}$ s and amplitude of ~ 140 kV [22–24] are discussed and interpreted within the framework of the mechanism of free electrons generation by means of interatomic Auger transitions.

1. Objects of study

As samples we used organofluorine and organosilicon liquids perfluoroeicosane, phenyl perfluoropentanoate (phenyl ester of perfluorovaleric acid), polydimethylsiloxane−200, as well as well-studied liquid dielectrics, such as transformer oil and ethanol. Organofluorine liquids were synthesized at the Institute of Organic Synthesis of the Ural Branch of the Russian Academy of Sciences.

The electronic structure of organic dielectric molecules is determined by the presence of covalent bonds involving sp^3-hybrid orbitals of the carbon atom [25]. Typical dielectrics of this class include alkanes, perfluoroeicosane, etc.

Perfluoroeicosane is a fluorine-substituted alkane with a relatively long chain of 20 carbon atoms. In perfluoroeicosane (Fig. 1, *a*) each carbon atom creates four σ-bonds

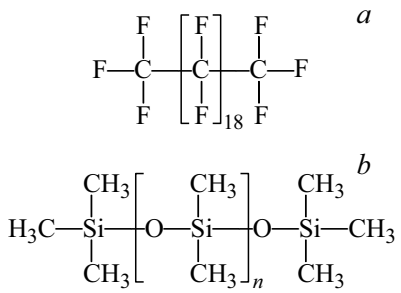

Figure 1. Single bonds of ions of carbon, silicon and oxygen in the structure of perfluoroeicosane (*a*) and polydimethylsiloxane−200 (*b*) molecules.

with neighboring atoms. The σ-bond itself is formed by the overlap of sp^3-hybridized orbitals, two with carbon atoms and two more with fluorine atoms. The covalent bond F−C forms due to $2p$-orbitals of fluorine and sp^3-orbitals of carbon. The energy spectrum of σ-electrons consists of levels filled and unfilled by electrons. Energy levels in organic materials are also called molecular orbitals. The highest occupied molecular orbital (HOMO) and the lowest unoccupied molecular orbital (LUMO) are separated by a forbidden band [25].

Long molecule of polydimethylsiloxane−200 (up to 200 monomers) is a silicon-oxygen chain with methyl groups attached to silicon atoms (Fig. 1, *b*) [26]. The covalent bond Si−O is formed due to sp^3-orbital states of silicon and $2p$-states of oxygen. The covalent bond gives the bonding and loosening orbitals of the molecule. Besides, the free $3d$-orbitals of silicon can take part in the formation of the silicon chemical bond. A donor-acceptor $d-p$-interaction occurs, which increases the bond order and reduces the Si−O interatomic distance.

The use of the band structure concept implies the presence of long-range and short-range order of the crystal lattice. It is the long-range order that provides the band character of the charge carriers motion in the crystal, in contrast to the hopping character in amorphous substances. The main role in determining the energy spectrum is played by the short-range order [27]. An example of the short-range order influence on the charge transfer properties can be found in paper [11]. The data from this paper show that the decrease in degree of short-range order in liquid in the case of mixing *n*-hexane and biphenyl reduces the drift mobility of electrons injected from the cathode from $\sim 4.2 \cdot 10^{-3}$ to $3.4 \cdot 10^{-3}$ cm^2/(V · s) at $E = 5$ kV/cm. The opposite process, i.e. increasing of short-range order degree, can lead to a situation where a quasicrystalline structure appears in an amorphous dielectric. For example, the ordering of long molecules if they are more or less parallel to each other [25]. The energy levels of the HOMO are put in correspondence to the upper edge of the valence band W_v, and of the LUMO — to the lower edge of the conduction band W_c.

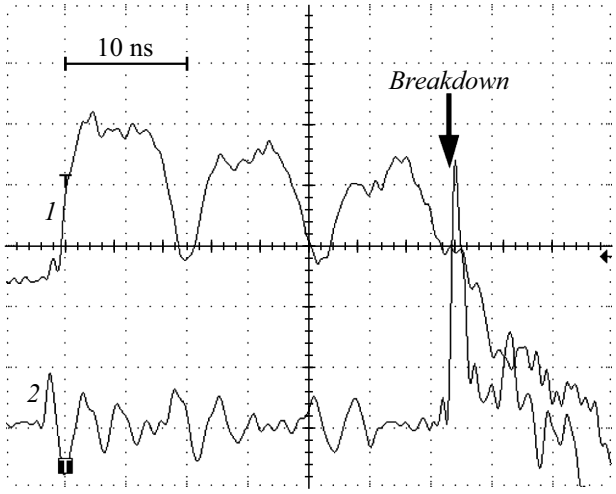

Figure 2. A typical oscillogram of voltage pulses on the needle electrode (*1*) and current through the sample (*2*).

The molecular model of naphthenic mineral oil [28] includes different types of alkanes: monocyclic $C_{14}H_{28}$ (32%), tricyclic $C_{16}H_{28}$ (26%), bicyclic $C_{13}H_{24}$ (18%), acyclic $C_{12}H_{26}$ (13%) and tetracyclic $C_{16}H_{26}$ (11%), which gives the density of $\sim 0.95\,g/cm^3$. Calculations of the electronic structure of mineral oil ab initio are presented in paper [28]. The valence and conduction bands of mineral oil are formed by the energy levels of the HOMO and LUMO states of alkane molecules, respectively. Forbidden band width is $\sim 6\,eV$.

2. Experimental procedure

The experimental setup includes a generator of high-voltage nanosecond pulses, a breakdown cell, and a Tektronix TDS 644B oscilloscope. The generator is a Tesla transformer built into a coaxial forming line with a sharpening hydrogen-filled spark gap. The spark gap working voltage is $\sim 140\,kV$. The pulse width when the generator runs at a matched load $Z = 50\,\Omega$ is 8 ns with rise time less than 0.5 ns. The measuring cell uses a point (anode) — plane (cathode) electrode configuration. The voltage pulse is applied to the anode. The distance between the electrodes d was adjusted with a screw. The dielectric sample in this electrical circuit is mismatched load for high-voltage generator, therefore, after the first voltage pulse, several reflected pulses with damped amplitude are observed until the moment of the complete breakdown of the dielectric (Fig. 2). The interval between reflected pulses is $\sim 2.8\,ns$, which is determined by the distance between the gas gap and the anode. The signals of the voltage across the gap and the discharge current through the sample were recorded simultaneously via two channels of the oscilloscope.

The breakdown time τ was assumed to be the interval between the moment of applying voltage to the sample and the moment of a sharp increase in current after the breakdown channel spans the interelectrode gap. The resulting breakdown time τ was determined as the average over 8−10 discharges. The velocity of breakdown channel propagation was calculated as $v_a = d/\tau$. The design of the pulse generator and the method for measuring the velocity of the breakdown channel propagation in liquid and solid dielectrics are described in more details in papers [22,24,29].

3. Results and discussion

Measuring the breakdown time τ at different lengths of the interelectrode gap in liquids using voltage pulse with rise time less than 0.5 ns makes it possible to estimate the velocity of breakdown channel formation and the dependence of velocity v_a on the electric field strength in the sample.

The change in the breakdown time τ and velocity v_a as a function of the gap distance d under the action of voltage pulse for the studied liquids is shown in Fig. 3. The breakdown time increases superlinearly with distance increasing between the electrodes. The extrapolation $\tau(d)$ (within the measurement error) passes through the origin of coordinates, which indicates that at high voltages there is no delay in the breakdown beginning with times more than 1−2 ns.

The highest velocities v_a correspond to samples of perfluoroeicosane and polydimethylsiloxane−200 ($3 \cdot 10^7$ and $2 \cdot 10^7$ cm/s), the lower velocities — to ethanol and transformer oil ($6 \cdot 10^6$ and $3 \cdot 10^6$ cm/s). The breakdown velocity decreases with d increasing (Fig. 3). The dependence of the breakdown velocity v_a on the electric field strength in the sample can be estimated by comparison of how the functions $v_a(d)$ and $E(d)$ change with the interelectrode distance d. The maximum field strength near the point E_m in the electrode structure „hyperboloid of revolution−plane“ is equal to [30]:

$$E_m = \frac{2U}{r \ln \frac{4d}{r}}, \qquad (1)$$

where r is the anode tip radius. For $r = 10\,\mu m$, $U = 140\,kV$ the estimate for $d = 0.5\,mm$ is $E_m = 5 \cdot 10^7$ V/cm. According to the terminology accepted in the literature [31] the average field strength in the sample is $E_{mid} = U/d = 2.8 \cdot 10^6$ V/cm, the field gain at the anode is $\beta = E_m/E_{mid} \approx 20$. The dependence of the electric field strength E_x on the coordinate x within the dielectric gap $(0-d)$ can be determined from expression [30]:

$$E_x = \frac{r}{r+x} E_m. \qquad (2)$$

The field E_x is heterogeneously distributed within the gap and is determined by the hyperbolic law. In the heterogeneous field, within the interval $(0-d)$ there is a point x_{mid}, where $E_x(x_{mid}) = E_{mid}$. This means that in the area from

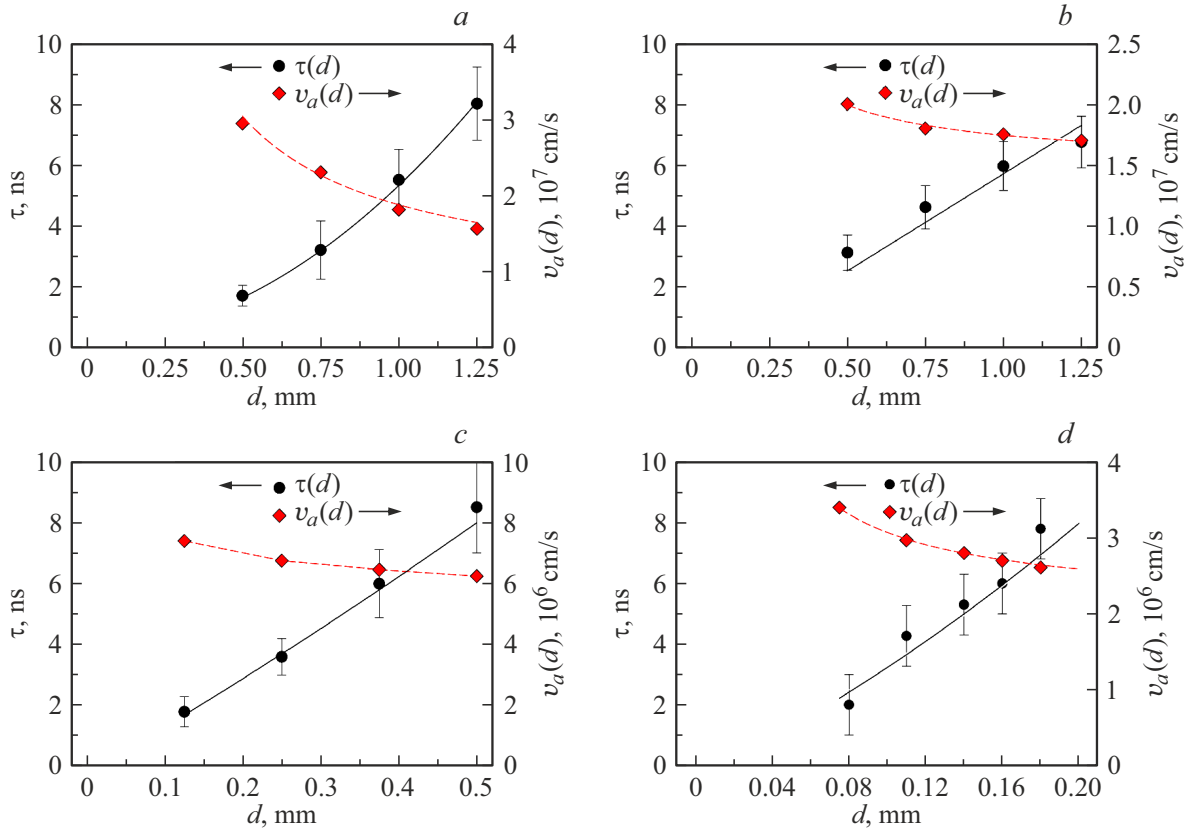

Figure 3. Formation time τ and the growth velocity of anode-initiated breakdown channel v_a vs. length of the interelectrode gap d for liquid samples: a — perfluoroeicosane; b — polydimethylsiloxane−200; c — ethanol; d — transformer oil.

the point electrode to the position x_{mid}, the strength is higher than E_{mid}, and in the area from x_{mid} to the plain electrode — lower. The value of this coordinate may be estimated as $x_{\text{mid}} \approx (0.2-0.3)d$. The nature of the change in breakdown channel velocity $v_a(d)$ depending on the length of the interelectrode gap for perfluoroeicosane and transformer oil agrees well with the hyperbolic dependence $E_{\text{mid}} \sim 1/d$. For polydimethylsiloxane−200 and ethanol, the curves of this dependence have more gently sloping character. It can be concluded that the breakdown velocity is proportional to the electric field strength with acceptable accuracy.

The measurement of the breakdown time of liquids for longer interelectrode gaps using three voltage pulses from a series of reflected pulses on the example of the phenyl perfluoropentanoate is shown in Fig. 4. It can be seen that the experimental points in the range up to 30 ns are satisfactorily approximated by line segments of power functions spaced by $\sim 3-4$ ns along the time axis. It can be assumed that the breakdown time τ in the region exceeding 8 ns includes a pause between pulses of 2.8 ns. This is possible provided that during the pause in the absence of applied voltage the channel retains increased conductivity. As in solid dielectrics [32], the channel grows deep into the sample with each sequentially arriving reflected pulse.

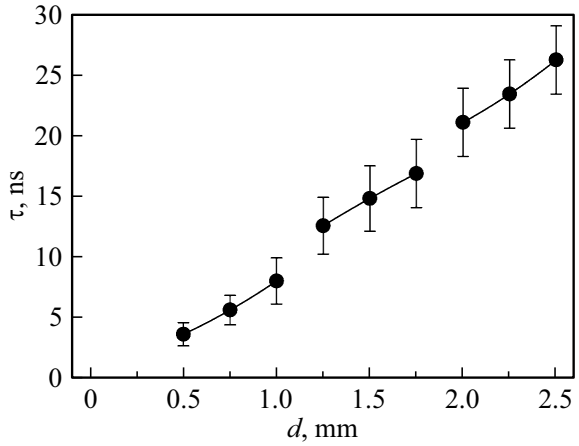

Figure 4. Breakdown time τ vs. the length of the interelectrode gap d for the values $\tau < 30$ ns for the phenyl perfluoropentanoate.

The values of the velocity of the breakdown channel propagation in perfluoroeicosane and polydimethylsiloxane−200 obtained in the experiment are comparable with those in single-crystal samples KBr and KCl, which under identical experimental conditions are $5 \cdot 10^7$ and $4.5 \cdot 10^7$ cm/s [29]. Probably, the factor determining the high velocity of breakdown channel propagation in these liquids is the structure

of their extended and highly ordered molecules. This quasi-crystalline feature of the liquid makes it possible to use theoretical ideas about the mechanism of initiation and propagation of the breakdown channel in solid dielectrics regarding the studied liquids.

4. Model of breakdown channel motion in perfluoroeicosane

The diagram of the energy bands in the region of contact between metal (electrode) and dielectric (perfluoroeicosane sample) in strong electric field is shown in Fig. 5.

According to papers [13,14] the beginning of the breakdown channel formation is determined by the processes at the „metal−dielectric" interface. At an average field strength in the sample of $\sim 10^6$ V/cm the real field strength near the electrode microprotrusions can be more than $\sim 10^8$ V/cm [33]. In the near-electrode region of the dielectric, due to the tunnel transition of electrons into the metal, the formation of F^{2+} ions with two holes in $2p$-orbitals takes place. For this, the required voltage U shall be such that the edge of the valence band of the dielectric will rise to the Fermi level of the metal. It is most likely that the neighboring carbon atom participates in the process of hole recombination by means of the interatomic Auger transition of the electron from sp^3-orbital of the C^0 atom to F^{2+} and subsequent generation of the Auger electron into the conduction band (Fig. 5, *a*). Hole recombination on C^{2+} (Fig. 5, *b*) is associated with the interatomic Auger transition of the electron from C^0 atom in the chain of carbon atoms of the perfluoroeicosane molecule. The transition of the Auger electron to the conduction band occurs under the condition that the minimum energy gap between the $2p$-orbitals F^{2+} and sp^3-orbitals of the atom C^0 and sp^3-orbitals of C^{2+} and C^0 atoms in the electric field is not less than the forbidden band of the dielectric.

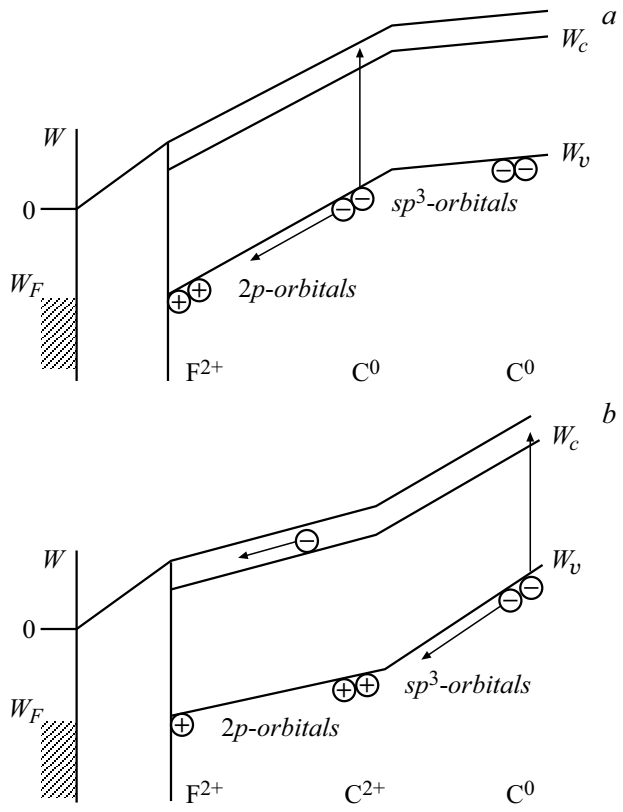

Figure 5. Scheme of cascade Auger transitions in perfluoroeicosane sample: *a* — near the metal−insulator interface; *b* — in the sample volume.

Issues related to the estimation of the electric field strength on the surface of the breakdown channel front are considered in relation to alkali halides in papers [13,14]. In alkali halides the required band bends for the Auger transitions are provided by the electric field of a space charge, which includes a layer of doubly charged halide ions and layers of singly charged ones [13,14]. The breakdown channel front coincides with the space charge boundary x_1 [14]. The electric field strength of the space charge dependence on time t in the region $x \geq x_1$ with the conductivity value $\sigma_0 = 0$ was obtained in [14]:

$$E_s(t) = \left(\frac{Ex_1}{x_2 - x_1} - \frac{G\Delta x^2}{(x_2 - x_1)\sigma_0}\right)\left(1 - \exp -\frac{t}{\tau_m}\right), \quad (3)$$

where σ_0 — breakdown channel conductivity, x_2 — sample length, $\tau_m = \varepsilon\varepsilon_0/\sigma_0$ — Maxwellian relaxation time, ε — dielectric permittivity of the sample, ε_0 — electric constant, G — volume velocity of the Auger electron charge generation in space from $x_1 - \Delta x$ to x_1, $\Delta x \sim 4$ Å — thickness of the atomic layer in the crystal, value $E = U/x_2$.

The single cycle of the space charge front movement can be divided into two successive stages. At the first stage, when the critical strength of the local electric field $\sim 10^8$ V/cm is reached, a hole decays due to the interatomic Auger transition of the electron from neighboring halogen atom, and the Auger electron is generated into the conduction band of the dielectric. The channel propagates by one interatomic distance. At the second stage the electrons are pulled out by the external electric field from the space charge region, and the critical field strength is reached for the implementation of the next cycle. Cycle time Δt can be represented as

$$\Delta t = \tau_A + \tau_1, \quad (4)$$

where $\tau_A \sim 10^{-16}$ s — the Auger transition time, τ_1 — time to reach the critical field strength. The time of establishment of the critical field strength can be defined as $\tau_1 = E_G/v_1$, where

$$E_G = \left(G\Delta x^2/(x_2 - x_1)\sigma_0\right)\left(1 - \exp(-\tau_A/\tau_m)\right)$$

— component of the field strength of Auger electrons in equation (3). Value

$$v_1 = \partial E_s/\partial t = \left(E_0 x_1/(x_2 - x_1)\tau_m\right)\exp(-t_0/\tau_m)$$

— field relaxation rate in the absence of generation. Time $t_0 \approx (1-2)\tau_m$. The duration of the single cycle of breakdown channel propagation is equal to

$$\Delta t = \tau_A + \frac{G\Delta x^2 \tau_m}{E x_1 \sigma_0} \exp\left(\frac{t_0}{\tau_m}\right)\left(1 - \exp\left(\frac{\tau_A}{\tau_m}\right)\right). \qquad (5)$$

According to (5), at high levels of conductivity and electric field strength E much higher than the electric strength of the dielectric E_b, the component τ_1 can become comparable or less than τ_A. In this case, the velocity of the the space charge boundary propagation $v(x_1) \approx \Delta x/\Delta t$ is determined by the time τ_A and is probably relatively stable with small change in E. According to [34] the value v_a in KCl single crystals at a voltage of 230 kV is $\sim 2 \cdot 10^8$ cm/s and does not change with the sample thickness in the range $d \sim 0.6-1.4$ mm. At the intensities $E \geq E_b$ the parameters of the breakdown channel propagation are mainly determined by the time τ_1. The velocity increases in proportion to E and σ_0, which is confirmed by experiments [18,19,29]. The presence of the coordinate x_1 in the denominator in formula (5) means the increase in space charge front velocity in the discharge gap $0-x_2$, which is observed experimentally according to photochronograms [19].

Probably, the breakdown channel in perfluoroeicosane is formed in the same way as described above. This is indicated by the initiation of the breakdown by the anode and the high value of the channel propagation velocity $\sim 3 \cdot 10^7$ cm/s. In accordance with the above model, the propagation of the breakdown channel front in perfluoroeicosane is associated with the positive charge transfer sequentially over the nearest carbon atoms and the generation of the Auger electrons into the conduction band of the dielectric (Fig. 5). Some of the electrons recombine with holes, releasing heat. The released energy is used to break chemical bonds and form free fragments of macromolecules, while thermal pressure forms a hollow channel with the gas phase. Macromolecules decompose into ions under the action of thermal collisions [29].

The structure of the breakdown channel is formed by a set of elementary one-dimentional channels of the Auger transitions (Fig. 5), passing in one direction. This structure includes a positive space charge and a conducting volume with a complex phase composition containing an electron-hole plasma. The channel front propagates from the positive electrode in the bulk of the sample. The channel diameter is probably determined by the size of the area within which F^{2+} ions layer is formed in the near-surface region of the dielectric, and its size is proportional to the external voltage. This regularity was observed earlier for KCl and KBr crystals, in which the breakdown channel diameter increased linearly with voltage in the range of 100−300 kV [19]. The formation time of the surface layer of F^{2+} ions according to the experimental data does not exceed 10^{-9} s.

According to the model of cascade Auger transitions, the condition for the initiation of the breakdown in the dielectric is the achievement of field strength at which the formation of near-electrode layer of positively charged ions (in particular, for perfluoroeicosane — F^{2+} ions) is possible through the electrons transfer from dielectric to metal. For this it is necessary to „raise“ by the electric field the upper edge of the valence band at least to the Fermi level of the metal W_F (Fig. 5). This requirement is met if the electric field strength near the electrode E_1 at an interatomic distance about $\Delta x \approx 1-2$ Å ensures the equality

$$E_1 \Delta x e = W_F - \varphi, \qquad (6)$$

where e — electron charge, φ — work function.

The electrical strength of the dielectric in „point−plane“ electrodes configuration can be represented as

$$E_b = E_1/\beta = (W_F - \varphi)/\Delta x e \beta.$$

According to the data of paper [24] the dielectric strength of perfluoroeicosane, measured in quasi-homogeneous field in the mode of slow voltage rise, is $E_b = 1.2 \cdot 10^5$ V/cm. Assuming $W_{F-\varphi} \approx 2$ eV, $\beta \approx 20$, we obtain the required field strength $E_1 \approx 10^8$ V/cm at which $E_b \approx 5 \cdot 10^6$ V/cm, which is realistic for the nanosecond mode of dielectric breakdown.

Conclusion

The paper shows that the highest velocities of breakdown channel propagation correspond to samples of liquids with long molecular chains (perfluoroeicosane, polydimethylsiloxane−200), and the lowest — to liquids with small molecules (transformer oil, ethanol). Probably, the level of liquid quasi-crystallinity is a factor that determines the breakdown velocity of liquid dielectrics. The presented qualitative model of the breakdown channel formation in perfluoroeicosane includes the mechanism of free electrons generation through the cascade Auger transitions in the valence band of the dielectric, heat release during the recombination of electron-hole pairs, and the formation of the gas-plasma phase. The model satisfactorily interprets the nature of the breakdown initiated by the positive electrode and the high velocity of the breakdown channel front propagation which is $\sim 10^7$ cm/s.

Conflict of interest

The authors declare that they have no conflict of interest.

References

[1] M.E. Savage, K.N. Austin, B.T. Hutsel, R.J. Kamm. *Proc. IEEE 21st Int. Conf. Pulsed Power* (UK, Brighton, 2017) DOI: 10.1109/PPC.2017.8291252

[2] S. Tkachenko, E.V. Grabovskii, A.V. Branitskii, I. Frolov, A. Gribov, A. Gritsuk, K. Mitrofanov, Y. Laukhin, G.M. Oleinik, A. Shishlov. *Proc. IEEE 21st Int. Conf. Pulsed Power* (UK, Brighton, 2017). DOI: 10.1109/PPC.2017.8291097
[3] J. Deng, W. Xie, S. Feng, M. Wang, H. Li, S. Song, M. Xia, J. Ce, A. He, Q. Tian, Y. Gu, Y. Guan, B. Wei, X. Huang, X. Ren, J. Dan, J. Li, S. Zhou, H. Cai, S. Zhang, K. Wang, Q. Xu, Y. Wang, Z. Zhang, G. Wang, S. Guo, Y. He, Y. Zhou, Z. Zhang, L. Yang, W. Zou. Matter Radiat. Extremes, **1**, 48 (2016). DOI: 10.1016/j.mre.2016.01.004
[4] *Sposob formirovaniya impul'sa toka v nagruzke induktivnogo nakopitelya elektromagnitnoi energii:* pat. 2746052 RF. Bazanov A.A.; № 2020126760; zayavl. 10.08.2020; opubl. 06.04.2021, Byul. № 10 (in Russian).
[5] G.A. Mesyats, I.V. Pegel'. *Vvedenie v nanosekundnuyu impulsnuyu energetiku i elektroniku* (FIAN, M., 2009), 192 s. (in Russian).
[6] G.A. Vorobyov, Yu.P. Pokholkov, Yu.D. Korolyov, V.I. Merkulov. *Fizika dielektrikov* (*oblast' silnykh polei), uchebnoe posobie* (Izda-vo TPU, Tomsk, 2003), 244 s. (in Russian).
[7] U. Mohan Rao, I. Fofana, A. Beroual, P. Rozga, M. Pompili, L. Calcara, K.J. Rapp. IEEE Tr. Dielectr. Electr. Insul., **27** (5), 1546 (2020). DOI: 10.1109/TDEI.2020.008765
[8] V.Ya. Ushakov, V.F. Klimkin, S.M. Korobeinikov, V.V. Lopatin. *Proboi zhidkostei pri impulsnom napryazhenii* (Izd-vo nauch.-tekh. lit-ry, Tomsk, 2005), 488 s. (in Russian).
[9] V.Ya. Ushakov. Izv. Tomsk. politekhn. un-ta, **307** (2), 80, (2004) (in Russian).
[10] V.F. Klimkin. Tech. Phys., **47** (9), 1106 (2002). DOI: 10.1134/1.1508185
[11] S. Sakamoto, H. Yamada. IEEE Tr. Electr. Insul., **EI-15** (3), 171 (1980). DOI: 10.1109/TEI.1980.298310
[12] H. Yamashita, H. Amano. IEEE Tr. Electr. Insul., **EI-20** (2), 247 (1985). DOI: 10.1109/TEI.1985.348827
[13] V.D. Kulikov. Tech. Phys., **54** (1), 56 (2009). DOI: 10.1134/S1063784209010083
[14] V.D. Kulikov. Tech. Phys., **57** (2), 192 (2012). DOI: 10.1134/S1063784212020144
[15] R.V. Emlin, S.V. Barakhvostov, V.D. Kulikov. Tech. Phys., **54** (7), 1076 (2009). DOI: 10.1134/S1063784209070275
[16] V. Kulikov, V. Yakovlev, L. Bobkova. NJDIS, **44** (1), 21 (2020).
[17] V. Kulikov. NJDIS, **62** (1), 51 (2021). DOI:10.24412/3453-9875-2021-62-1-51-54
[18] A.A. Vorobyov, G.A. Vorobyov. *Electricheskiy proboi i razrushenie tverdykh tel* (Vysshaya shkola, M., 1966), 224 s. (in Russian).
[19] Yu.N. Vershinin. *Elektronno-teplovye i detonatsionnye protsessy pri elektricheskom proboe tverdykh dielektrikov* (UrO RAN, Ekaterinburg, 2000), 260 s. (in Russian).
[20] H. Yamada, S. Kimura, T. Sato. *Proc. 3rd Int. Conf. Conduction and Breakdown in Solid Dielectrics* (Trondheim, Norway, 1989), p. 87, DOI: 10.1109/ICSD.1989.69167
[21] G.A. Mesyats. *Pulsed Power* (Kluwer Academic/Plenum Publishers, NY., 2004)
[22] I.F. Punanov, R.V. Emlin, P.A. Morozov, S.O. Cholakh. Russ. Phys. J., **55** (2), 191 (2012). DOI: 10.1007/s11182-012-9794-5
[23] I.F. Punanov, R.V. Emlin, P.A. Morozov, S.O. Cholakh. *Proc. IEEE 21st Int. Conf. Pulsed Power* (Brighton, UK, 2017), DOI: 10.1109/PPC.2017.8291194
[24] I.F. Punanov. *Prostranstvenno-vremennye i energeticheskie kharakteristiki vysokovoltnogo nanosekundnogo proboya kondensirovannykh dielektrikov* (Dis. kand. fiz.-mat. nauk. Yekaterinburg, UrFU, 2017) (in Russian).
[25] J.E. Spice. *Chemical Binding and Structure* (Pergamon Press, NY., 1964)
[26] *Oligoorganosiloksany. Svoystva, poluchenie, primenenie*, pod. red. M.V. Sobolevskiy (Khimiya, M., 1985), 264 s. (in Russian).
[27] V.L. Bonch-Bruevich, S.G. Kalashnikov, *Fizika poluprovodnikov* (Nauka, M., 1977), 672 s. (in Russian).
[28] C. Bin, D. Ji-Wei, Ch. Ming-He. Crystals, **11** (2), 123 (2021). DOI: 10.3390/cryst11020123
[29] I.F. Punanov, R.V. Emlin, V.D. Kulikov, S.O. Cholakh. Tech. Phys., **59** (4), 503 (2014). DOI: 10.1134/S1063784214040197
[30] J.M. Meek, J.D. Craggs. *Electrical Breakdown of Gases* (Clarendon Press, Oxford, 1953), 507 p.
[31] G.A. Mesyats. JETP Lett., **85** (3), 109 (2007). DOI: 10.1134/S0021364007020038
[32] R.V. Emlin, I.F. Punanov. Phys. Solid State, **59** (8), 1565 (2017). DOI: 10.1134/S1063783417080108
[33] G.A. Mesyats. Dokl. Phys., **49** (12), 727 (2004). DOI: 10.1134/1.1848625
[34] R.V. Emlin, Yu.N. Vershinin, V.A. Beloglazov. *Tr. IX Simposiuma po silnotochnoy elektronike. Nikolaev 21–30 iyulya 1992.* (Nauch.-tekh. redaktsiya „Giperoks", M., 1992), s. 299. (in Russian).